Contents

I. Physical measurements

The FT-IR spectrum was performed using KBr pellet by a WQF-520A FT-IR spectrometer. The powder X-ray diffraction (PXRD) patterns were prepared by DX-2700 X-ray diffractometer. The solid UV-Vis diffuse reflectance spectrum was measured by Agilent Cary 5000 spectrophotometer at environment temperature. Spectra were typically measured in the range of 230-900 nm. Mass spectra were recorded on a high-resolution Fourier transform ICR spectrometer with Bruker maXis Quadrupole Time-of-Flight (QTOF) mass spectrometry in positive mode. The TGA curve was recorded using a Q50 Thermogravimetric device with 10 °C/min in the nitrogen atmosphere. Luminescence was measured by a Hitachi F-7000 spectrometer. X-ray photoelectron spectroscopy (XPS) was recorded on PHI Quantum-2000. The sample was put under UHV to reach the 10^{-8} Pa range. The nonmonochromatized Al Kα source was used at 10 kV and 10 mA. All binding energies were calibrated using the C (1s) carbon peak (284.6 eV), which was applied as an internal standard. High resolution narrow-scan spectra were recorded with the electron pass energy of 50 eV and takeoff angle of 55° to achieve the maximum spectral resolution.

X-ray Crystallography. Intensity data of **Ag_6** and **$Ag_6(0)\cdot Ag_6(I)$** were collected on an a Bruker SMART APEX CCD diffractometer at 293 K (Cu Kα) and 100 K (Mo Kα), respectively. Absorption corrections were applied by using the program CrysAlis (multi-scan). The structures were solved by direct methods, and non-hydrogen atoms were refined anisotropically by least-squares on F^2 using the SHELXTL program.

Electron counting. According to the counting rules introduced by Mingos and Häkkinen,[1,2] the three silver clusters can be considered as superatom complexes formulated as $[L_S{\cdot}A_NX_M]^z$ with electron-withdrawing ligands X or weak Lewis base ligands L attached to the core with metal atoms A and an overall core charge z. Accordingly, for Ag the 5s electrons are counted and corrected by the number of electrons that are located at electron-withdrawing ligands and corrected by

the charge of the cluster. Ligands *L* (3S in this work) are "weak ligands" and do not affect the effective free-electron-count of the silver core. In this regard, the free electron *n** of the three clusters can be evaluated with a formula:

$$n^* = Nv_A - M - q$$

M is the number of electron-withdrawing ligands, *N* is the number of metal atoms, an "effective metal valence" $v_A = 1$, *q* means the overall charge of the cluster.

As a result, the shell-closing electron number *n** of **Ag_6(0)** with a formula $[Ag_6(3S)_4(OTf)_4]$ is 2, *n** of **Ag_6(I)** with a formula $[Ag_6(3S)_4(C{\equiv}C^tBu)_4]^{2+}$ is zero, while **Ag_6** with a formula $[Ag_6(3S)_4(tfa)_4]$ is also a 2-electron superatom.

II. Synthesis

Materials and reagents.

T-butyl acetylene (^{t}BuC≡CH, 98%), 1,3,5-trithiane (3S, 97%), Triethylamine (TEA, 99.0%) were purchased from J&K; Silver Trifluoromethanesulfonate (AgOTf, 98%) and Silver trifluoroacetate (Agtfa, 98%) were purchased from TCI and other reagents employed were purchased from Sinopharm Chemical Reagent Co. Ltd. (Shanghai, China). $(AgC{\equiv}C^tBu)_n$ was prepared by reacting of Ag_2O and ^{t}BuC≡CH in the presence of ammonium hydroxide.[3] All reagents were used as received.

Caution! Due to the explosive nature of silver alkynyls, great care should be taken and only small amounts should be used.

$[Ag_6(3S)_4(OTf)_4]\{[Ag_6(3S)_4(C{\equiv}C^tBu)_4](OTf)_2\}$, $Ag_6(0)\cdot Ag_6(I)$

$(AgC{\equiv}C^tBu)_n$ (57 mg, 0.3 mmol) was dissolved in CH_3CN (5 mL) of Ag(OTf) (77 mg, 0.3 mmol) under ultrasonication, then **3S** (41.5 mg, 0.3 mmol) was added creating a clear solution. The resulting solution was sealed in a 20 mL screw-top glass bottle and heated to 70 ℃ for 20 h. After cooled to room temperature, the light-yellow solution was filtered. The colorless hexagonal crystals were achieved by slow evaporation of the filtrate at 5 ℃ for 2 weeks. Yield: 10.3 mg, 5.5% based on Ag.

Anal. UV-Vis (λ, nm): 237 (ε = 8.1 x 10^4 L.mol^{-1}.cm^{-1}), 326 (ε = 2.9 x 10^4 L.mol^{-1}.cm^{-1}) in THF; 272, 352 in the solid state. ESI-MS (DMF): 1646.11 ($[Ag_6(3S)_4(OTf)_3]^+$) and 1241.78 ($Ag_{14}(C{\equiv}C^tBu)_{12}]^{2+}$). IR (KBr, ν, cm^{-1}): 1023, 1257, 1169 and 1222 (OTf^-), 2034 (C≡C), 3005−2866, 1391, 730 (3S). XPS (binding energy, eV): Ag $3d_{5/2}$, 367.6; Ag $3d_{3/2}$, 373.6 eV. Emission in the solid state: Em = 499, 603 nm (should peak), Quantum yield: 16.4%. Lifetime: τ=93.97±0.46 μs, for 499 nm; τ_1=58.35±0.83 μs (57.93%); τ_2=132.25±2.32 μs (42.07%) for 603 nm.

$Ag_6(3S)_4(tfa)_4$, Ag_6

Ag(tfa) (132.6 mg, 0.6 mmol) was dissolved in CH_3CN (5 mL) under ultrasonication, then **3S** (41.5 g, 0.3 mmoL) was added to form a clear solution. Then TEA (42 μL, 0.3 mmol) was added. The resulting solution was sealed in a 20 mL screw-top glass bottle and heated to 70 ℃ for 20 h. After cooled to room temperature, the colorless block crystals were obtained directly by filtration. Yield: 42 mg, 25% based on Ag.

Anal. UV-Vis (λ, nm): 252 (ε = 3.2 x 10^4 L.mol^{-1}.cm^{-1}), 306 (ε = 4.2 x 10^4 L.mol^{-1}.cm^{-1}) in THF; 253, 305 in the solid state. ESI-TOF-MS (DMF): 1538.26 ($[Ag_6(3S)_4(tfa)_3]^+$). IR (KBr, ν, cm^{-1}): 1699 and 1199 (tfa^-), 3029−2866, 1386, 720 (3S). XPS (binding energy, eV): Ag $3d_{5/2}$, 367.8; Ag $3d_{3/2}$, 373.8 eV. Emission in the solid state: Em = 526 nm, Quantum yield: 14.0%. Lifetime: τ_1=6.64±0.07 μs (38.71%); τ_2=167.66±1.74 μs (61.29%).

III. DFT calculations

Density functional theory (DFT) calculations were performed with the quantum chemistry program Gaussian 16.[4] Molecular structures from X-ray structural determination were adopted as the calculation models after structural optimization. The 6-31G(d) basis set was used for C, H, O, S, P, and LANL2DZ for Ag.[5] Geometry optimizations were performed with the B3LYP functional, and time-dependent DFT calculations of the UV-vis absorption spectrum were performed with the PBE0 functional.[6] One hundred singlet states (nstates = 100, singlet) are chosen in the calculations of the UV-Vis absorption spectra.

1. D. Michael, P. Mingos, *Polyhedron* **1984**, *3*, 1289-1297.
2. H. Häkkinen, *Chem. Soc. Rev.* **2008**, *37*, 1847-1859.
3. (a) K. G. Liu, F. Bigdeli, H. J. Li, J. Z. Li, X. W. Yan, M. L. Hu, and A. Morsali, *Inorg. Chem.* **2020**, *59*, 6684–6688. (b) K. G. Liu, X. W. Wei, F. Bigdeli, X. M. Gao, J. Z. Li, X. W. Yan, M. L. Hu, and A. Morsali, *Inorg. Chem.* **2020**, *59*, 2248–2254.
4. M. J.Frisch, G. W.Trucks, H. B.Schlegel, G. E.Scuseria, M. A.Robb, J. R.Cheeseman, G.Scalmani, V.Barone, G. A.Petersson, H.Nakatsuji, X.Li, M.Caricato, A. V.Marenich, J.Bloino, B. G.Janesko, R.Gomperts, B.Mennucci, H. P.Hratchian, J. V.Ortiz, A. F.Izmaylov, J. L.Sonnenberg, D.Williams-Young, F.Ding, F.Lipparini, F.Egidi, J.Goings, B.Peng, A.Petrone, T.Henderson, D.Ranasinghe, V. G.Zakrzewski, J.Gao, N.Rega, G.Zheng, W.Liang, M.Hada, M.Ehara, K.Toyota, R.Fukuda, J.Hasegawa, M.Ishida, T.Nakajima, Y.Honda, O.Kitao, H.Nakai, T.Vreven, K.Throssell, J. A.Montgomery Jr, J. E.Peralta, F.Ogliaro, M. J.Bearpark, J. J.Heyd, E. N.Brothers, K. N.Kudin, V. N.Staroverov, T. A.Keith, R.Kobayashi, J.Normand, K.Raghavachari, A. P.Rendell, J. C.Burant, S. S.Iyengar, J.Tomasi, M.Cossi, J. M.Millam, M.Klene, C.Adamo, R.Cammi, J. W.Ochterski, R. L.Martin, K.Morokuma, O.Farkas, J. B.Foresman and D. J.Fox, Gaussian 16, Revision B.01, Gaussian Inc., Wallingford CT, **2016**.
5. (a) P. J. Hay and W. R. Wadt, *J. Chem. Phys.* **1985**, *82*, 299-310; (b) A. D. Becke

Phys. Rev. A **1988**, *38*, 3098-3100.
6. D. Coskun, S. V. Jerome and R. A. Friesner, *J. Chem. Theory Comput.* **2016**, *12*, 1121-1128.

IV. Supporting figures

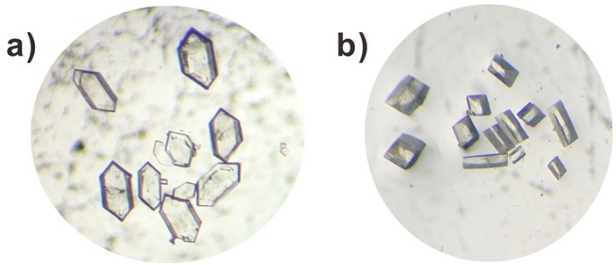

Figure S1. Optical image of a) **$Ag_6(0)\cdot Ag_6(I)$** and b) **Ag_6** (right).

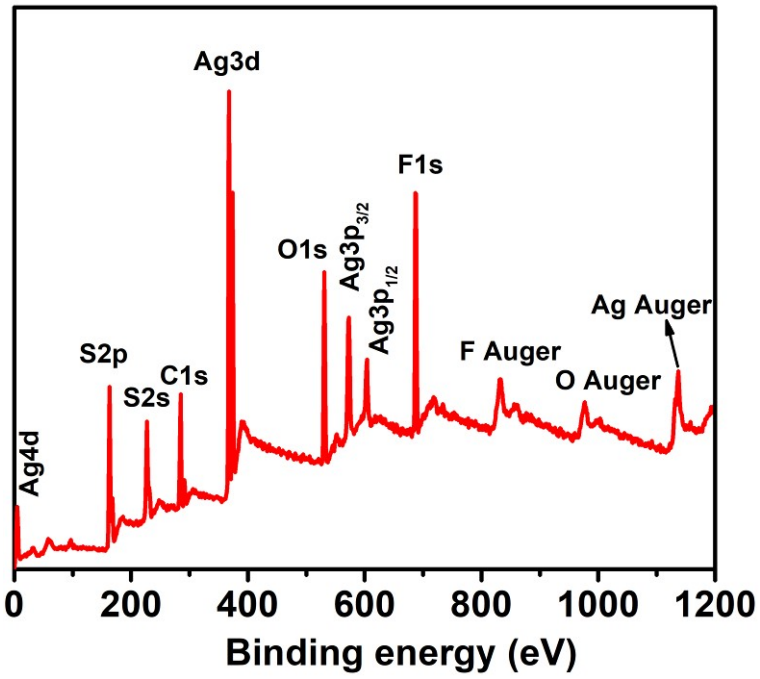

Figure S2. XPS of **$Ag_6(0)\cdot Ag_6(I)$**.

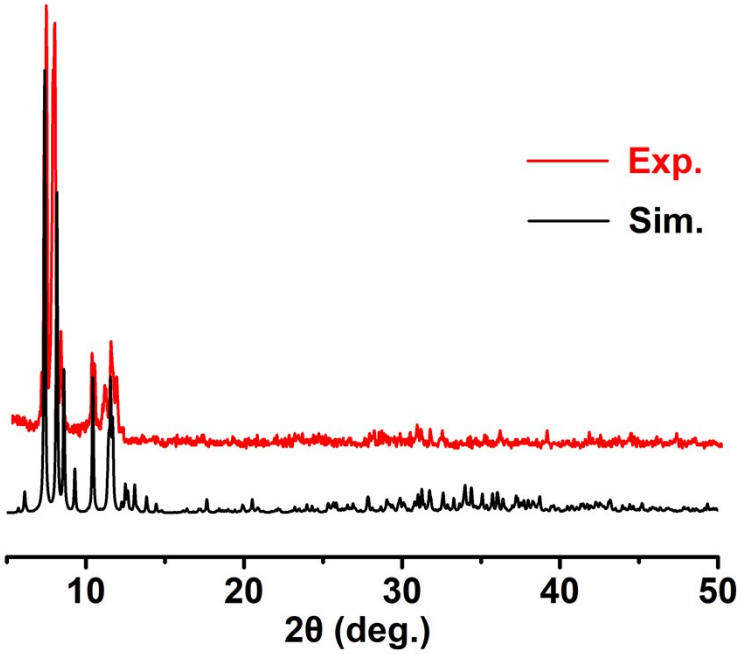

Figure S3. The experimental and simulated PXRD spectra of **Ag_6(0)·Ag_6(I)**.

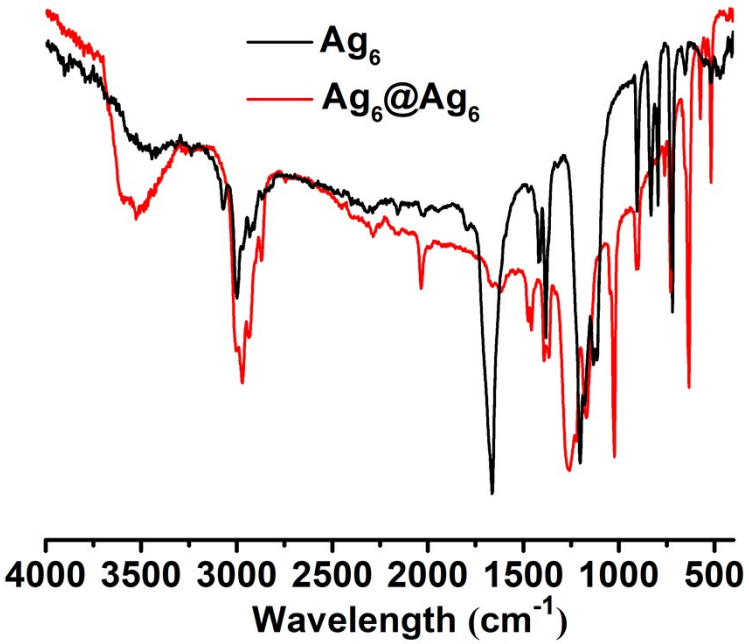

Figure S4. IR spectrum of **Ag_6(0)·Ag_6(I)** (red trace) and **Ag_6** (black trace).

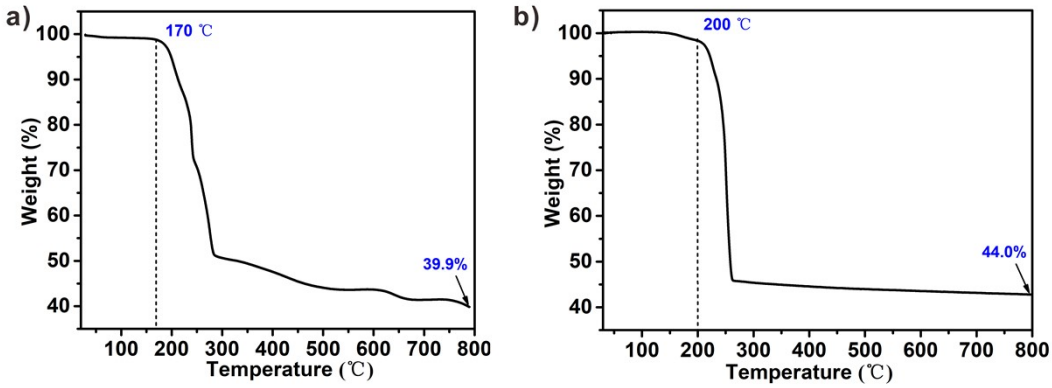

Figure S5. Thermogravimetric analysis (TGA) of **$Ag_6(0)\cdot Ag_6(I)$** (left) and **Ag_6** (right) in N_2 atmosphere.

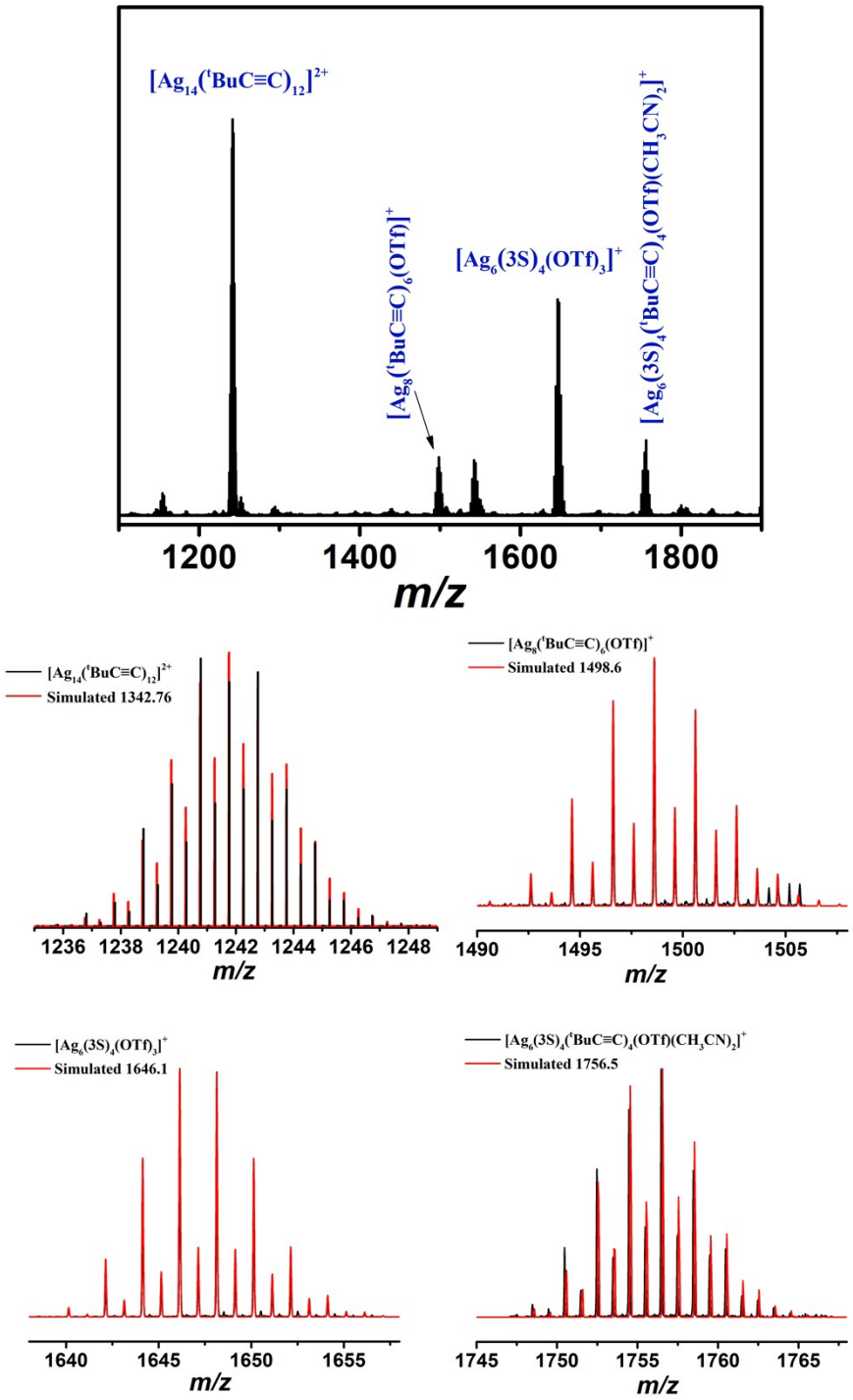

Figure S6. Mass spectra and the analysis of the four dominating peaks of **$Ag_6(0)\cdot Ag_6(I)$** in THF.

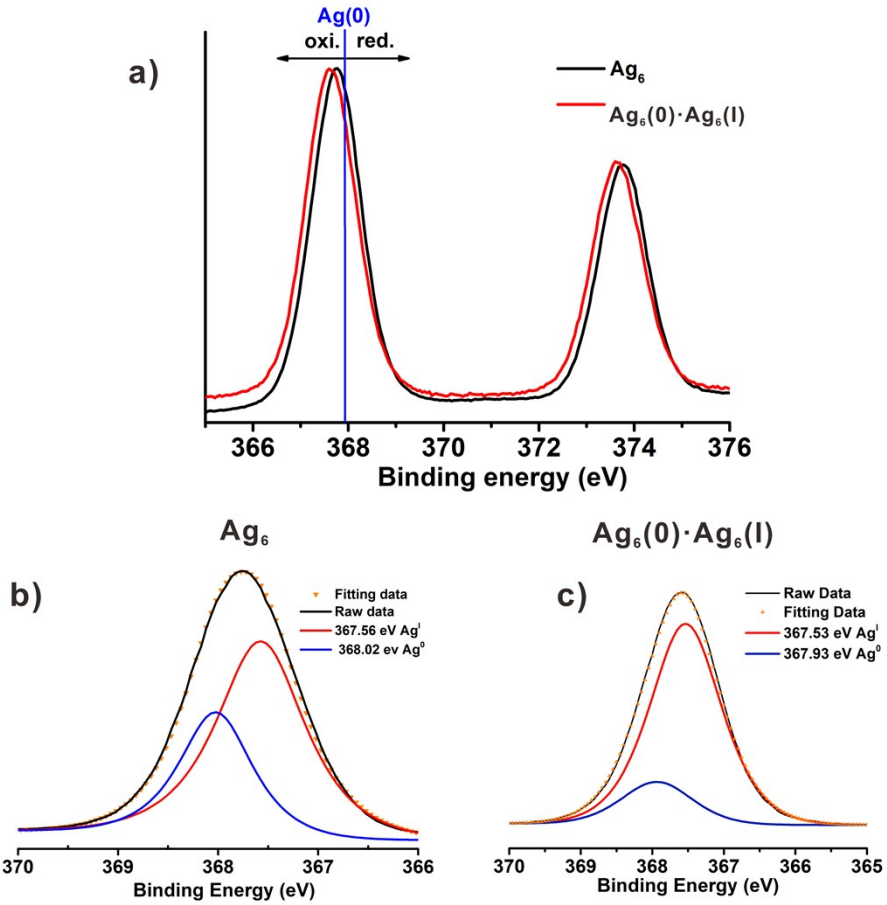

Figure S7. a) XPS of the expanded Ag 3d regions in **$Ag_6(0)\cdot Ag_6(I)$** (red trace) and **Ag_6** (black trace). The Ag $3d_{5/2}$ peaks of b) **Ag_6** and c) **$Ag_6(0)\cdot Ag_6(I)$** were fitted for Ag(0) and Ag(I) peaks.

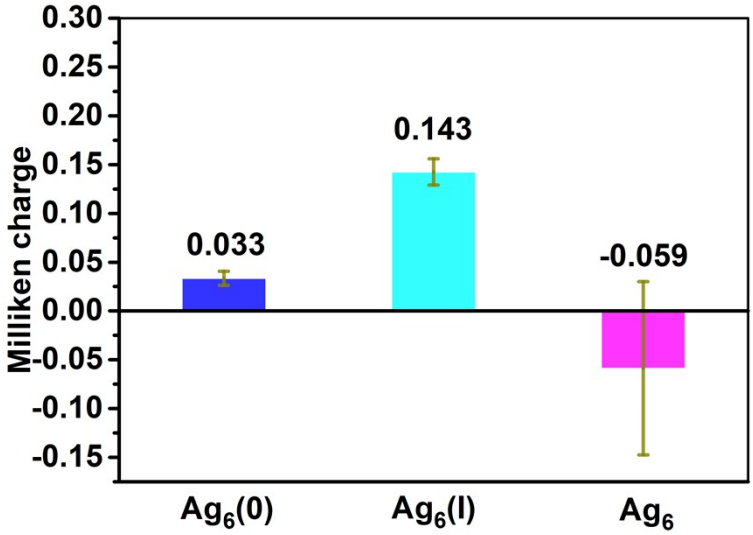

Figure S8. Average Milliken charges of the Ag atoms in **Ag_6(0)**, **Ag_6(I)** and **Ag_6**.

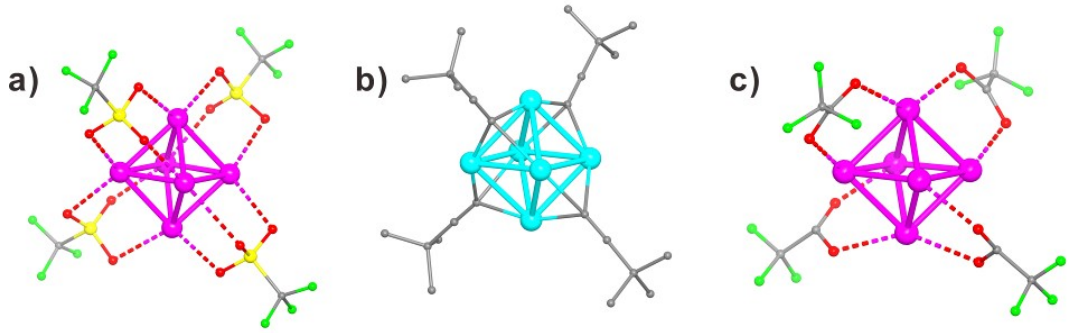

Figure S9. Structure comparation of a) **Ag_6(0)**, b) **Ag_6(I)** and c) **Ag_6** showing the coordination mode of OTf^-, $^tBuC{\equiv}C^-$ and tfa^- ligands, respectively.

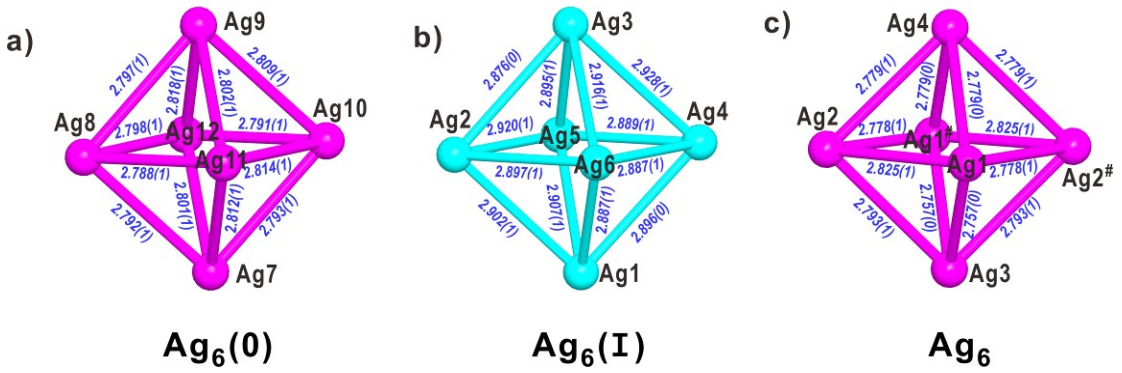

Figure S10. Ag-Ag distance comparation of the octahedral Ag_6 core in **Ag_6(0)**, **Ag_6(I)** and **Ag_6**.

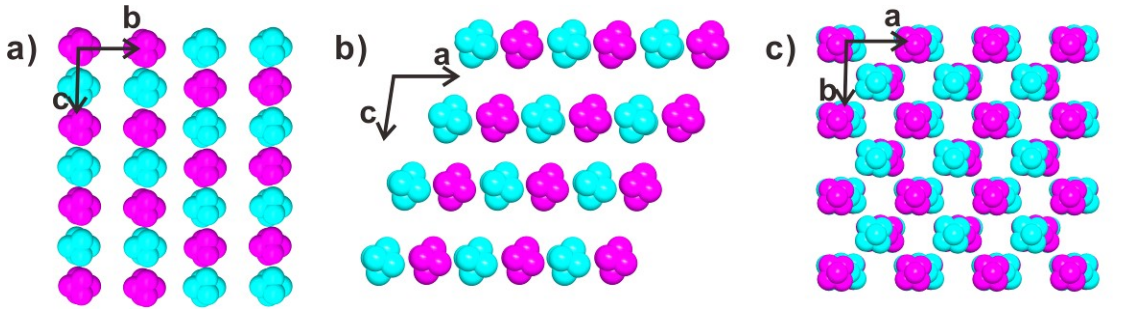

Figure S11. Packing of **Ag_6(0)** and **Ag_6(I)** clusters in the crystal lattice, viewed along the (a) a-axis, (b) b-axis, and (c) c-axis. Ag purple **Ag_6(0)**, Ag light blue **Ag_6(I)**. All the ligands are omitted for clarity.

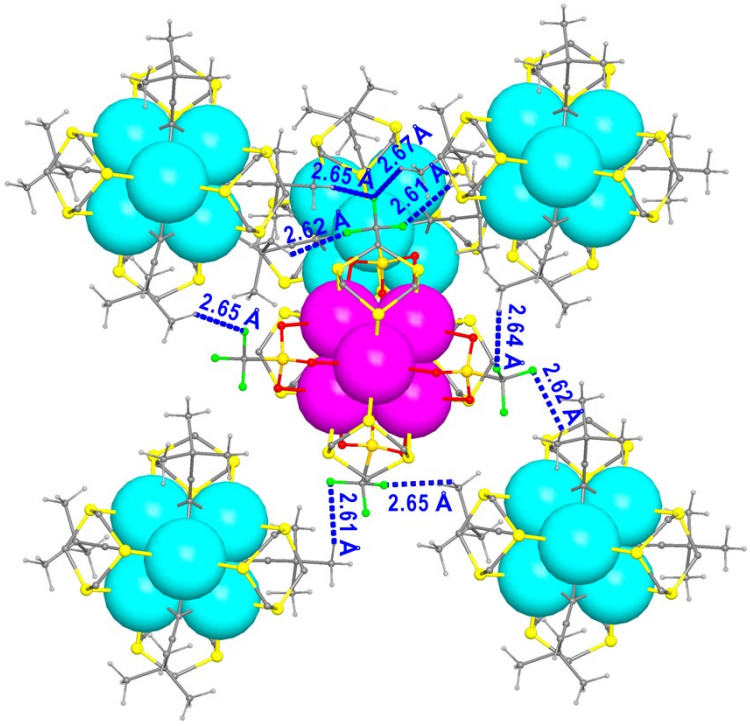

Figure S12. Illustration of the intercluster interactions in **Ag_6(0)** and **Ag_6(I)** clusters via C-H (^{t}BuC≡C$^-$)···F (OTf$^-$) hydrogen-bonds.

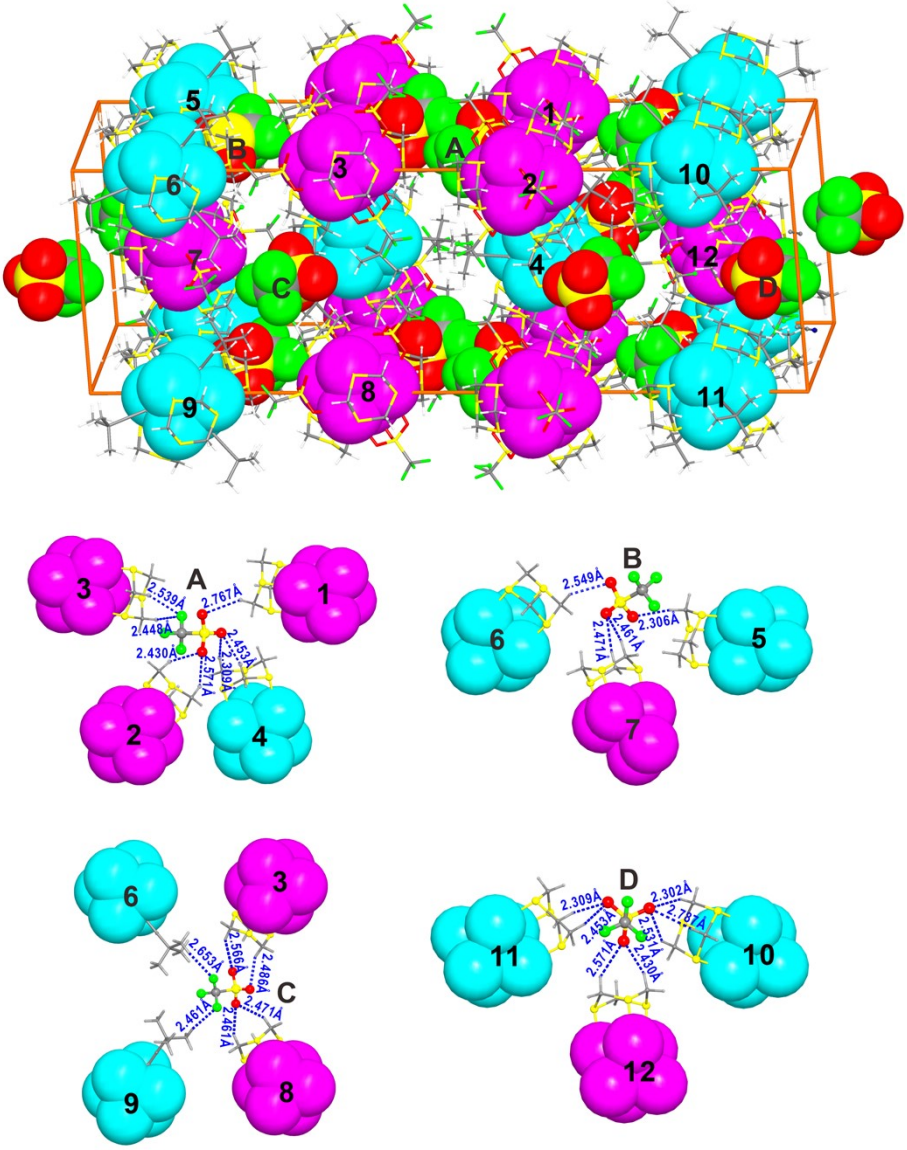

Figure S13. Coordination geometry of the crystallographically independent triflate anions showing the different C−H···O and C−H···F multiple hydrogen-bonding modes.

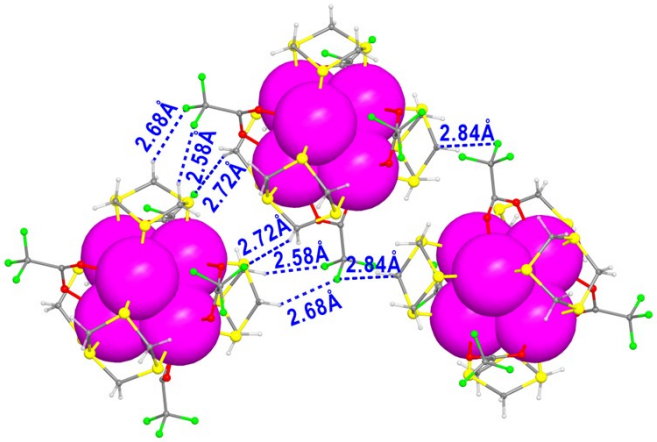

Figure S14. The intermolecular interactions in **Ag_6**. The intercluster C–H (3S)···F hydrogen bonds are in the range of 2.58-2.84 Å.

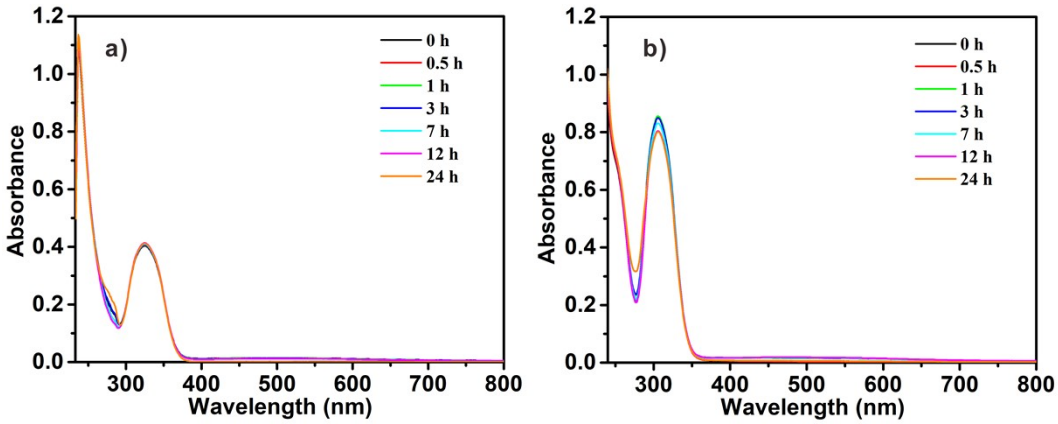

Figure S15. Time-dependent UV−vis spectrum of (a) **$Ag_6(0)\cdot Ag_6(I)$** and (b) **Ag_6** in THF.

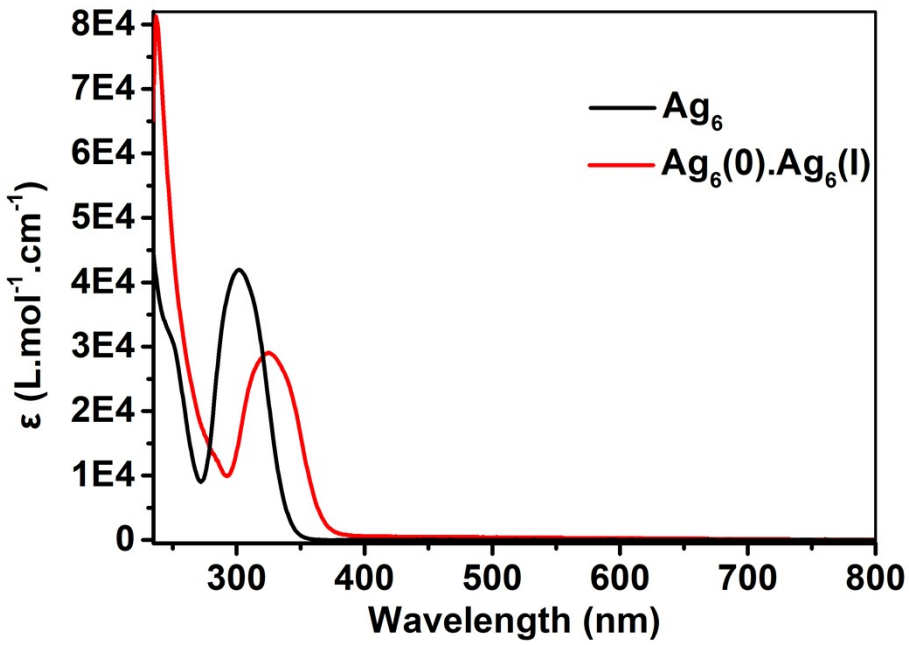

Figure S16. UV−vis spectrum of **Ag_6(0)·Ag_6(I)** and **Ag_6** in THF.

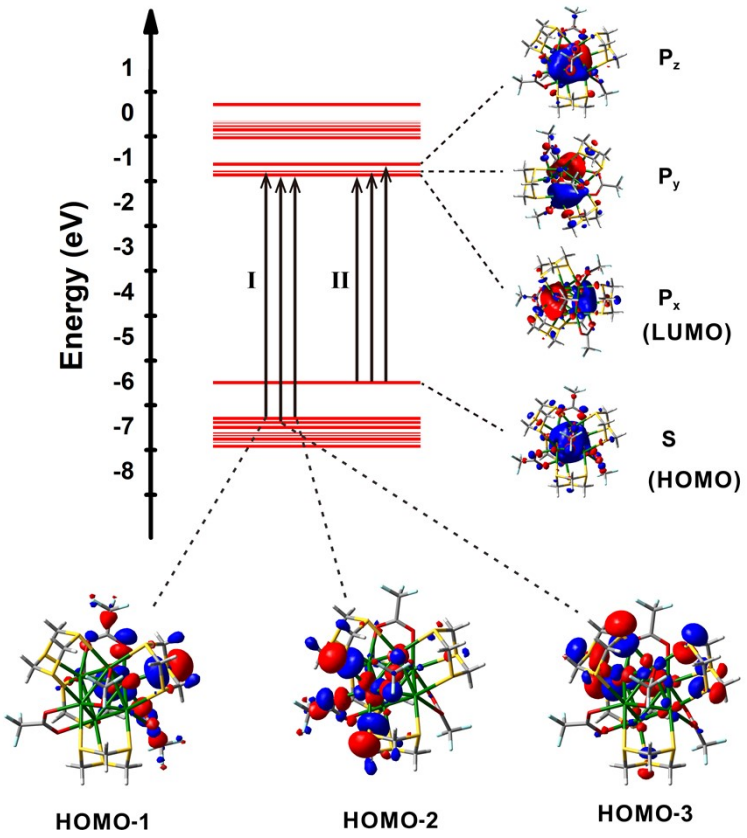

Figure S17. Energy-level correlation diagram and the orbitals involved in the transitions of **Ag_6**.

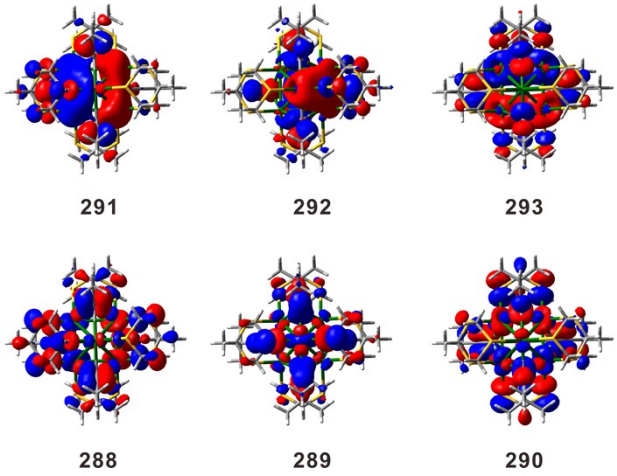

Figure S18. The frontier orbital of **Ag_6(I)**. 288-290 are triple degenerated HOMO orbitals, while 291-293 are three degenerate LUMO orbitals.

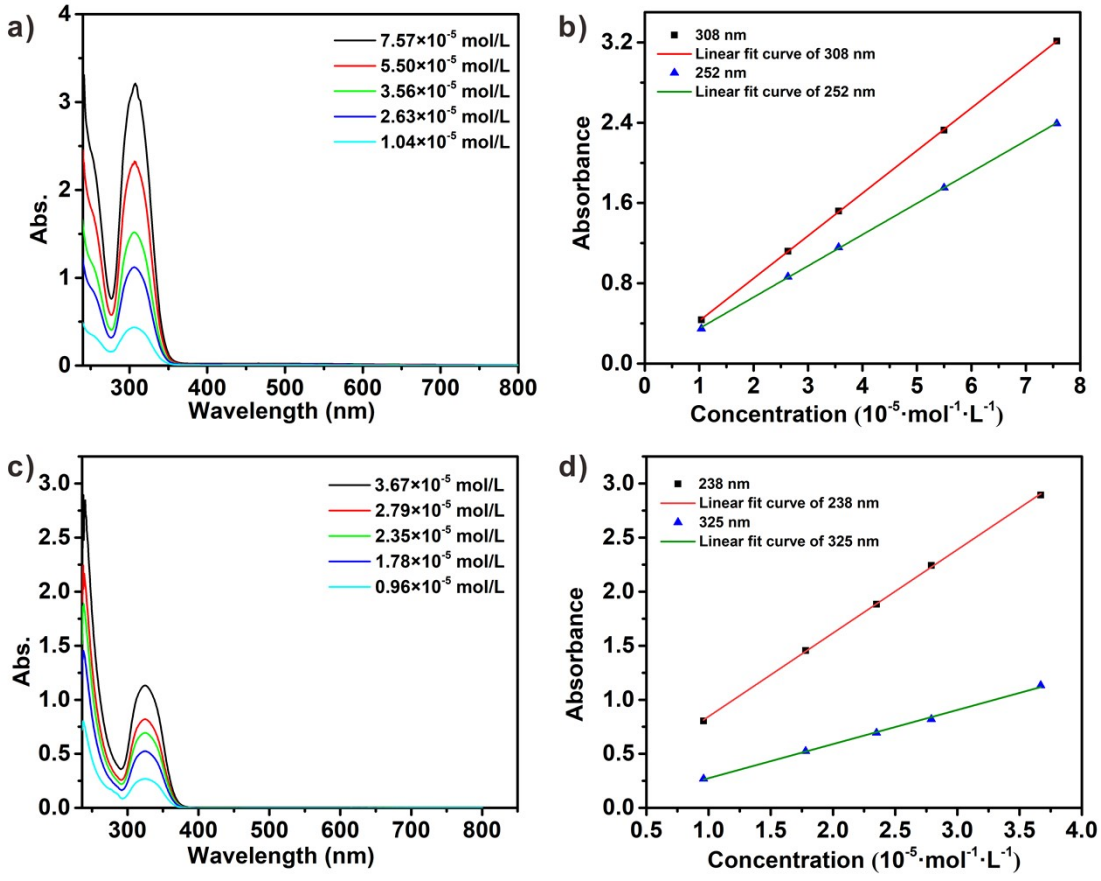

Figure S19. The absorption spectrum of a) **Ag_6** and c) **Ag_6(0)·Ag_6(I)** in THF solution by varying their concentration. The correlation between concentration and absorption intensity of b) **Ag_6** and d) **Ag_6(0)·Ag_6(I)** at various wavelengths.

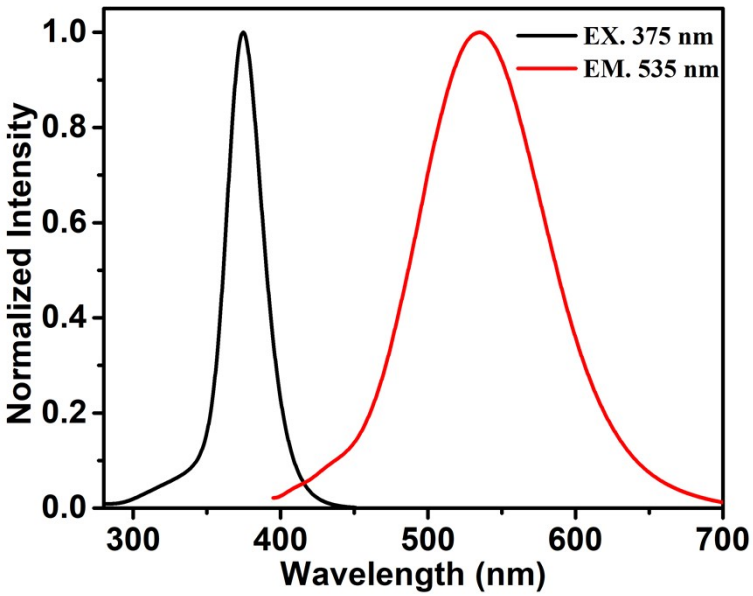

Figure S20. Excitation and emission spectra of **$Ag_6(0)\cdot Ag_6(I)$** in THF.

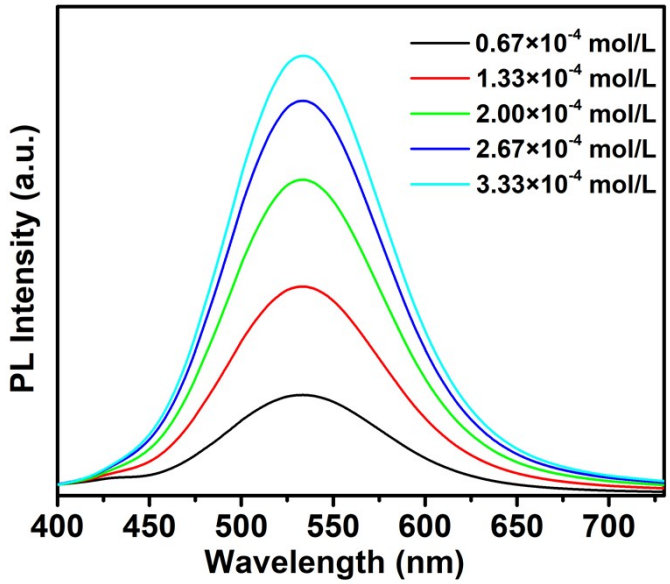

Figure S21. PL spectra of **$Ag_6(0)\cdot Ag_6(I)$** in THF with different concentration. Ex = 375 nm.

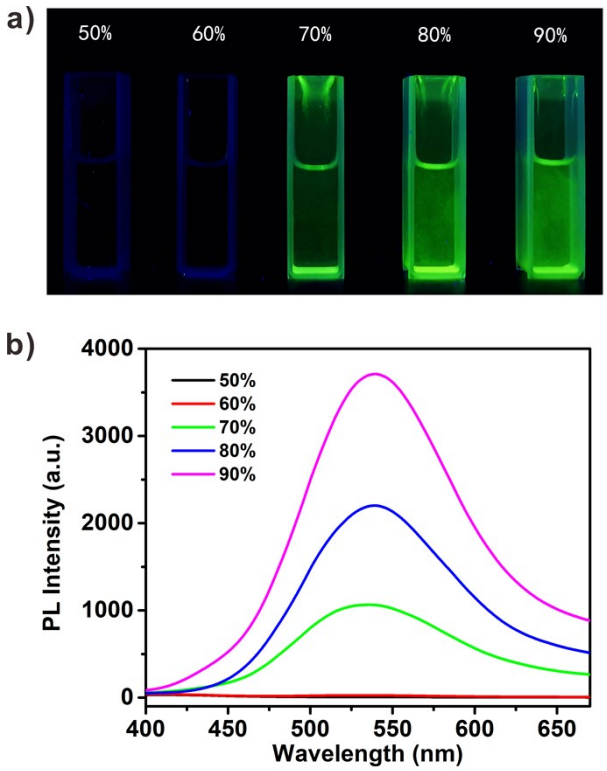

Figure S22. (a) Fluorescence photographs of $\mathbf{Ag_6}$ in THF solution with different fractions of Et_2O under UV 365 nm. (b) The AIE activities of $\mathbf{Ag_6}$ in with different volume ratios of Et_2O in the THF/Et_2O mixture excitated at 375 nm.

Table S1. Crystal data and structure refinement for **Ag_6** and **$Ag_6(0)\cdot Ag_6(I)$**.

Compounds	**Ag_6**	**$Ag_6(0)\cdot Ag_6(I)$**
Chemical formula	$C_{20}H_{24}O_8F_{12}S_{12}Ag_6$	$C_{60}H_{93}N_3O_{19}F_{18}S_{30}Ag_{12}$
Formula weight	1652.33	3758.76
Crystal system	Monoclinic	Monoclinic
Space group	*C*2/*c*	$P2_1/n$
a, Å	26.1584(5)	15.6815(6)
b, Å	10.02650(10)	15.1285(5)
c, Å	19.8095(4)	48.3672(19)
α, deg	90	90
β, deg	128.008(3)	98.4260(10)
γ, deg	90	90
V, Å^3	4093.72(18)	11350.7(7)
Z	4	4
ρ_{calc}, g/cm^3	2.681	2.194
μ, mm^{-1}	29.221	2.658
Reflections collected	51335	123526
Independent reflections	4128	32340
R_{int}	0.0425	0.0400
Reflections I > 2σ(I)	4075	25427
Parameters	274	1301
GOF on F^2	1.057	1.032
$R_1{}^a/wR_2{}^b$ (I > 2σ(I))	0.0349/0.0916	0.0534/0.0978
$R_1{}^a/wR_2{}^b$ (*all*)	0.0355/0.0920	0.0727/0.1040

Table S2. Selected bond lengths (in angstrom) of **Ag_6(0)**, **Ag_6(I)** and **Ag_6** from DFT/PBE calculations. Experimental values are listed in parentheses for comparison.

Bond		**Ag-Ag**	**Ag-S**	**Ag-O /Ag-C**
Ag_6(0)	Exp.	2.7880(6)-2.8175(6) 2.801	2.5826(14)-2.6381(16) 2.611	2.592(1)-3.146(1) 2.859
	Cal.	2.913-2.931 2.920	2.785-2.806 2.799	2.672-2.809 2.734
Ag_6(I)	Exp.	2.8759(5)-2.9282(5) 2.900	2.6229(14)-2.7570(14) 2.674	2.263(1)-2.357(1) 2.302
	Cal.	3.049-3.065 3.058	2.905-2.983 2.947	2.326-2.341 2.334
Ag_6	Exp.	2.7568(5)- 2.8249(5)2.785	2.5959(12)-2.7819(14) 2.672	2.406(1)-2.793(1) 2.579
	Cal.	2.834-2.948 2.884	2.769-3.038 2.883	2.441-2.576 2.483

Table S3. Experimental and computed peak positions (in nm) in the optical absorption spectra.

Cluster	Peak	TDDFT	Exp.
$Ag_6(0)\cdot Ag_6(I)$	i	238	237
	ii	314	326
Ag_6	I	260	252
	II	308	306